Journal of Engineering Physics and Thermophysics, Vol. 69, No. 5, 1996

THERMAL MODEL OF LOCAL ULTRASOUND HEATING OF BIOLOGICAL TISSUE

V. A. Nedogovor, V. L. Sigal, and
E. I. Popsuev

UDC 576.8.06

Possibilities of creation of controlled temperature fields in deep-seated biological tissue with the use of an endocavity ultrasound applicator with surface cooling are considered. Mathematical models are proposed and calculated that make it possible to construct acoustic and thermal fields in biotissues depending on the thermophysical and ultrasound characteristics of the medium being irradiated and to reveal situations and effects that are important for solving problems of practical medicine in the field of local ultrasound hyperthermia and thermotherapy of tissue.

The need to design compact ultrasound emitters for controlled endocavity heating of the biological tissue is determined by particular problems of modern theoretical and clinical local hyperthermia and thermotherapy [1, 2]. Despite certain advances in this field of practical medicine, first and most of all historically connected with the use of microwave (MW) radiation for local hyperthermia, a number of important circumstances revealed in recent years require not only new and improved electromagnetic methods and heating devices, but also fields of other physical nature for controlled heating. This is especially important since the specific effect of an MW field, aside from its thermal action, is still unclear [3]. In essence, mechanisms of the selective action of particular temperatures on normal and tumor cells which determine the therapeutic effects of methods of local hyperthermia are still not revealed.

The controlled ultrasound (US) heating of tissues has, in contrast to MW fields, certain advantages based on the physical features of ultrasound [4] which should manifest themselves during nonivasive thermal action on deep-seated tissues and tumors that do not have boundaries with gas cavities or bone tissue. Among these are, first of all, various mechanical and thermal phenomena in biological tissues and cell membranes, changes in their permeability, phonophoresis, etc. The small size of the focused beam (the wavelength of ultrasound vibrations with a frequency of 0.5–3 MHz in soft tissue is 3–0.3 mm) and relatively weak attenuation of the beam (about 1 dB/cm/MHz in muscle tissue [5, 6]) determine extremely important, from the viewpoint of practical biomedical therapeutic applications of ulrtasound hyperthermia and biodestruction, possibilities for more-precise focusing of the radiation at a considerable controlled depth of energy transport in a conducting medium, controlling the energy release and configuration of acoustic fields, etc. Evidently, these factors have stimulated few investigations that give grounds for application of methods of local ultrasound hyperthermia and thermotherapy to the treatment of a number of malignant pathologies that are not treated successfully by MW fields. For example, in [7] this is stated regarding the treatment of prostate cancer using the endocavity local hyperthermia.

It is evident that the creation of a controlled thermal distribution in a particular region of tissue, especially deep-seated tissue, is not only a problem for special medical devices, still not designed, but also a subject of mathematical modeling.

The formulation of a mathematical model is determined, first of all, by the presence of an ultrasound field structure around an emitter placed in a natural human-body cavity formed by biotissue.

The compound acoustic pressure induced by a source of harmonic vibrations at a certain point is determined by the Rayleigh–Sommerfeld integral [8]

Kiev Polythechnical Institute, Kiev, Ukraine. Institute of Experimental Pathology, Oncology, and Radiobiology, National Academy of Sciences of Ukraine, Kiev, Ukraine. Translated from Inzhenerno-Fizicheskii Zhurnal, Vol. 69, No. 5, pp. 779-784, September-October, 1996. Original article submitted July 24, 1995.

 1062-0125/96/6905-0596$15.00

$$P(r) = \frac{j\rho ck}{2\pi} \int_S u(\bar{r}') \frac{\exp(jk|\bar{r} - \bar{r}'|)}{|\bar{r} - \bar{r}'|} dS . \quad (1)$$

The possibilities of local ultrasound irradiation of tissue are determined by the near-field zone $x_{nf} \leq L^2/\lambda$, i.e., when the maximum linear dimension of the source is $L = 10$ mm and $\lambda = 1.5$ mm, we have $x_{nf} \leq 70$ mm. This means that the distribution of the radiation intensity has a compound, interference character, in contrast to the simple exponential distribution proposed in [9], which takes place during irradiation of extremely thin tissue layers (about 3 mm) in the vicinity of the applicator and does not meet the requirements of practical medicine.

In this connection, calculation of $P(\bar{r})$ by Eq. (1) in the near field can be carried out by representing the emitter S as a superposition of elementary square emitters [10] with area $\Delta S = \Delta h \times \Delta w$:

$$P(x, y, z) = \frac{j\rho c}{\lambda} \sum_{n=1}^{N} u_n \int_{-\Delta h/2}^{\Delta h/2} \int_{-\Delta w/2}^{\Delta w/2} \frac{\exp(-(\alpha + jk) r)}{r} dx_0 dy_0 ;$$

$$r = \sqrt{z^2 + (x - x_n - x_0)^2 + (y - y_n - y_0)^2} .$$

It is evident that for uniformly excited vibrations (a model of an oscillating piston) the value of amplitudes and phases of the vibration velocity are equal for all the elementary emitters.

We use the Fraunhofer approximation, according to which for any x_0 and y_0 the following condition is satisfied:

$$x_0 << R ; \quad y_0 << R , \quad R = \sqrt{z^2 + (x - x_n)^2 + (y - y_n)^2} .$$

Inasmuch as

$$\frac{kx_0^2}{2R} + \frac{ky_0^2}{2R} << \pi ; \quad \alpha << R ; \quad \frac{1}{r} \approx \frac{1}{R}$$

and

$$\exp\left(\frac{\alpha x_n' x_0}{R}\right) \approx 1 \quad \text{when} \quad \frac{\Delta w}{2} > x_0 > -\frac{\Delta w}{2} ;$$

$$\exp\left(\frac{\alpha y_n' y_0}{R}\right) \approx 1 \quad \text{when} \quad \frac{\Delta h}{2} > y_0 > -\frac{\Delta h}{2} ,$$

then, after simple transformations we obtain the final expression for calculations

$$P(x, y, z) = \frac{j\rho c \Delta S}{\lambda} \sum_{n=1}^{N} \left[\frac{u_n}{R} \exp(-(\alpha + jk) R) \operatorname{sinc} \frac{kx_n' \Delta w}{2R} \operatorname{sinc} \frac{ky_n' \Delta h}{2R} \right] . \quad (2)$$

Thus, the distribution of the field in the near zone for a rectangular emitter can be calculated in terms of the vector sum of the distributions of the field in the far zone for elementary rectangular sources subject to the following inequality [10]:

$$\max(\Delta w, \Delta h) \leq \sqrt{\left(\frac{4\lambda z_{min}}{F}\right)} . \quad (3)$$

Usually, the value of the parameter $F = 10-15$ [10]. At these values of F the relative error of calculation of the sound pressure δP does not exceed 2–5% at distances $z \geq z_{min}$. Thus, for calculation of the radiation intensity of

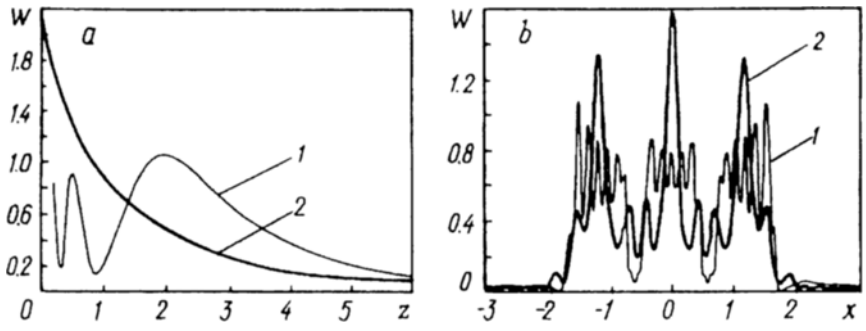

Fig. 1. Distribution of specific ultrasound power W in biotissue: a) over biotissue depth on the main axis of the applicator from three emitters for vibrational velocities of plates $u_1 = 0$, $u_2 = 16$ cm/sec, $u_3 = 0$ (curve 1) and for a cylindrical emitter calculated according to [9] for emitter radius $r_0 = 1.2$ cm and vibrational velocity $u = 16$ cm/sec (curve 2); b) as a function of the distance from the symmetry axis of the applicator at vibrational velocities $u_1 = 0$, $u_2 = 16$ cm/sec, $u_3 = 0$ for depths of 0.2 cm and 1.8 cm, curves 1, 2, respectively. W, W/cm^3; z, cm; x, cm.

the applicator, we take the size of an elementary source to be equal $\Delta w \times \Delta h = 0.108 \times 0.108$ cm, the ultrasound wavelength $\lambda = 0.15$ cm, and the parameter $F = 12$ ($\delta P \approx 3\%$ at $z = z_{min}$). Then, according to (3), $z_{min} \approx 2$ mm, i.e., the given method provides sufficient accuracy of calculation within virtually the entire region of interst, excluding the extremely thin surface layer where the US intensity can be considered equal to that on the applicator surface.

Using (2) we can calculate the power $W(x, y, z)$ released in a unit volume of biotissue by the formula

$$W(x, y, z) = \frac{|P(x, y, z)|^2}{\rho c} \alpha . \tag{4}$$

The squared absolute value of the amplitude of the sound pressure can be found using (2). In practical applications, Eq.(2) is transformed from complex to trigonometric form and substitued into (4).

Thus, the squared amplitude of the sound pressure for an endocavity ultrasound emitter consisting of three identical rectangular emitters placed in a row can be calculated out by the following formula:

$$P(x, y, z) = \left\{ -\frac{\rho c \Delta S}{\lambda} \sum_{i=1}^{I} u_i \left\langle \sum_{m=1}^{M} \sum_{n=1}^{N} \left[\frac{\exp(-\alpha R_{imn}) \sin(kR_{imn})}{R_{imn}} \operatorname{sinc} \frac{kx'_{im} \Delta w}{2R_{imn}} \operatorname{sinc} \frac{ky'_{in} \Delta h}{2R_{imn}} \right] \right\rangle \right\}^2 +$$

$$+ \left\{ \frac{\rho c \Delta S}{\lambda} \sum_{i=1}^{I} u_i \left\langle \sum_{m=1}^{M} \sum_{n=1}^{N} \left[\frac{\exp(-\alpha R_{imn})}{R_{imn}} \cos(kR_{imn}) \operatorname{sinc} \frac{kx'_{im} \Delta w}{2R_{imn}} \operatorname{sinc} \frac{ky'_{in} \Delta h}{2R_{imn}} \right] \right\rangle \right\}^2 .$$

Results of calculation of the ultrasound pressure in biotissue are illustrated by Fig. 1. In these calculations the frequency of US vibrations was 1.05 MHz, the dimensions of the emitter 1 × 1 cm (three in a row), and the US attenuation coefficient in the tissue 0.136 cm^{-1}. It follows from the calculations that the intensity distribution of the ultrasound is oscillating both in depth (Fig. 1a) and parallel to the emitter surface (Fig. 1b). In the near zone the character of the distribution of the ultrasound field calculated by the method of the rectagular emitter differs substantially from the intensity of the ultrasound field of a cylindrical emitter calculated in [9] (Fig. 1a). It is evident that the latter method is valid only for heating of the surface region of tissue. The most pronounced maximum of the radiation intensity is observed on the main axis of the emitter at a distance of about 1.8 cm from its surface (Fig. 1a). It can be assumed that the thermal field pattern will also have alternating maxima and minima. An appreciable temperature maximum should be expected at a depth of 1.5–2.0 cm on the main axis of the emitter.

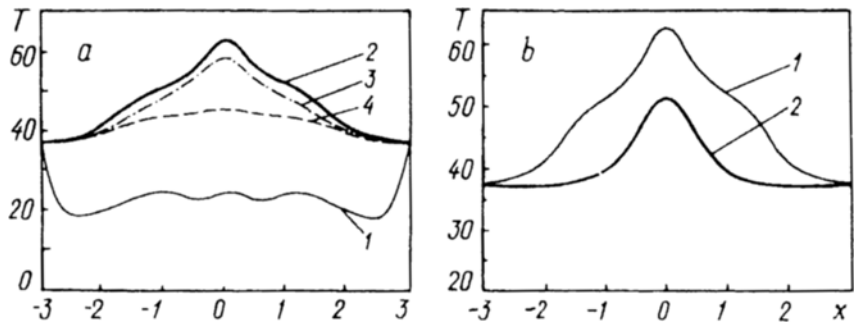

Fig. 2. Temperature distribution in biotissue as a function of distance from the symmetry axis of the applicator at cooling temperature $T_{cl} = 15^{\circ}C$ and bloodflow $w_b = 0.45 \cdot 10^{-5}$ m^3/kg·sec: a) for depths of 0.5 cm, 1.8 cm, 2.5 cm, and 4 cm (curves 1-4, respectively) at vibrational velocities $u_1 = u_2 = u_3 = 16$ cm/sec; b) for a depth of 1.8 cm at vibrational velocities $u_1 = u_2 = u_3 = 16$ cm/sec (curve 1) and $u_1 = 0$, $u_2 = 16$ cm/sec, $u_3 = 0$ (curve 2). T, °C.

We use the obtained power $W(x, y, z)$ released in a unit volume of biotissue to build temperature fields $T(x, y, z)$ as solutions of the classical biothermal equation in a cylindrical coordiante system [1, 2, 11]. For the applications under consideration the latter can be written as follows:

$$\frac{\partial^2 T}{\partial r^2} + \frac{1}{r}\frac{\partial T}{\partial r} + \frac{\partial^2 T}{\partial z^2} + \frac{1}{k_t} W(r, z) - C(T - T_b) = \frac{1}{\alpha}\frac{\partial T}{\partial t}. \tag{5}$$

In (5) we neglect metabolic heat production, since during local hyperthermia and especially during thermotherapy a much more powerful heating source is acting.

The boundary conditions for (5)

$$-k_t \frac{\partial T}{\partial r} + KT = KT_{cl}, \quad r = r_2, \quad t > 0;$$

$$T = T_b, \quad r = \tilde{n} r_2, \quad t \geq 0; \quad T = T_b, \quad t = 0 \tag{6}$$

take into account the possibility of cooling of the emitter surface. We can assume that cooling affects the temperature distribution in the vicinity of the applicator, where rather high temperature values can be observed. This makes it possible to prevent, if necessary, burning of the biotissue and to heat more deep-seated volumes of the tissue.

It is evident that at a certain distance from the emitter ($\tilde{n} \approx 5-10$) the tissue temperature $T = T_b$, which is also taken into account by conditions (6).

The coefficient K determines in fact the efficiency of the cooling system, and its value very strongly reflects the heat transfer between the cooling liquid and the biological tissue. The choice of K is determined, e.g., in [11], and depends on the specific thermal conductivity of this liquid but when certain relationships between the dimensions of the channels in laminar flow are satisfied does not depend on its velocity.

A numerical solution of the biothermal equation (5) was obtained by the finite-element method [12, 13] for specific values of thermophysical, ultrasound, and perfusion parameters of the medium being irradiated (Figs. 2, 3).

An analysis of results of calculations has shown that already at a vibrational velocity of the emitter surface equal to 16 cm/sec (the admissible value for piezoceramics) controlled temperatures sufficient even for thermodestruction can be achieved in tissue. At depths of the order of 0.5–1 cm, the effect of cooling of the applicator on the temperature of the tissue is still appreciable (Fig. 2a, curve 1). In this case the temperature distribution along the applicator (at the same excitation intensity) has three maxima, in accordance with the number

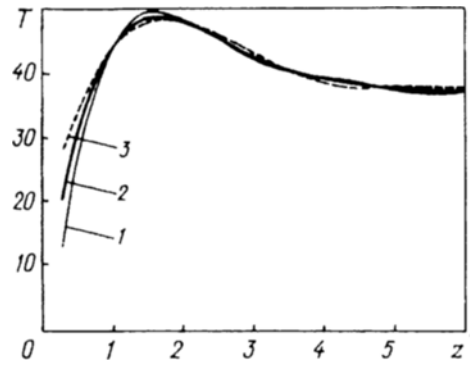

Fig. 3. Temperature distribution over depth of biotissue on the main axis of the applicator from three emitters at vibrational velocities $u_1 = u_2 = u_3 = 16$ cm/sec, bloodflow $w_b = 0.45 \cdot 10^{-5}$ m^3/kg·sec for cooling temperatures: T_{cl} = 10°C, 15°C, and 25°C (curves 1-3, respectively).

of elements. The maximum temperature is achieved at a depth 1.9 cm on the main axis of the applicator (Fig. 2a, curve 2), which corresponds approximately to the position of the zone of maximum specific ultrasound power. At distances from the applicator of up to 3 cm (Fig. 2a, curves 2 and 3), a more and more pronounced temperature maximum is observed on the main axis of the applicator; at a distance equal to 4 cm and greater (Fig. 2a, curve 4) this maximum "spreads out." By comparing the distribution of the specific ultrasound power (Fig. 1b) with the temperature field, one can notice a very strong "smoothing" effect of heat transfer in the tissue.

It has been found that the depth of the temperature maximim depends weakly on the cooling temperature of the applicator surface and is determined primarily by the position of the maximum of the specific ultrasound power. A change in the cooling temperature affects the tissue temperature only at distances of 0–1.5 cm (Fig. 3).

When instead of the three plates of the applicator just one of them is turned on (Fig. 2b, curve 2), this results in not only narrowing of the heated zone but also a substantial decrease in the temperature both at the maximum point (for the conditions under consideration, by about 10°C) and within the entire zone of action of the applicator.

Thus, ultrasound fields have rather high flexibility and specificity of action on biotissue, provide rather sufficient possibilities for deep penetration, and, in order to create controlled thermal fields, make it possible to achieve a wide range of temperatures.

The work was supported by the State Committee of Ukraine on Problems of Science and Technologies.

NOTATION

P, compound acoustic pressure; $\bar{r}$, vector that determines the position of the point of the field at which pressure P is determined; $\bar{r}'$, vector that determines the position of a point on the emitter surface; S, area of the emitter; u, component of the vibration velocity normal to S; ρ, density of the medium; c, velocity of sound in the medium; $k = 2\pi/\lambda + j\alpha$, wavenumber; λ, wavelength in the medium; α, attenuation coefficient of ultrasound in the medium; x_{nf}, length of the near-field zone of the emitter; L, maximum linear dimension of the emitter; ΔS, area of elementary emitter; Δh and Δw, dimensions of elementary emitter in plane; x, y, and z, coordinates of the point at which P is determined; x_n and y_n, coordinates of the center of elementary source; x_0 and y_0, current coordinates in system related to elementary source; N, number of elementary emitters into which the source is divided; u_n, vibrational velocity of the n-th elementary source; R, distance between center of elementary source and point at which P is determined; sinc $(X) = \sin(X)/X$; z_{min}, minimum distance from source plane to point at which P is calculated provided that the error does not exceed the permissible value; F, parameter that determines the relative error δP of calculation of sound pressure; I, number of rectangular emitters, components of multi-element applicator; i, number of rectangular emitter; x'_{im} and y'_{in}, current coordinates of the center of the mn-th elementary portion of the i-th emitter; R_{imn}, distance from a point (x, y, z) in the field to the mn-th element of the i-th emitter;

u_i, vibrational velocity on the surface of the i-th emitter; W, specific power of ultrasound in biotissue; $\alpha' = k_t/\rho_t c_t$; k_t, ρ_t, and c_t, specific thermal conductivity, density, and specific heat of the tissue, respectively; $C = C_b \rho_b m_b \rho_t / k_t$; C_b, specific heat of blood; m_b, volume flow per unit tissue weight; T_b, temperature of blood entering the heated area (arterial blood temperature); r_2, radius of surface being cooled; T_{cl}; temperature of cooling liquid; K, integral heat transfer coefficient.

REFERENCES

1. M. Gautherie (ed.), Interstitial, Endocavity, and Perfusional Hyperthermia: Methods and Clinical Trials, Berlin (1991).
2. G. H. Nussbaum (ed.), Physical Aspects of Hyperthermia, (1982).
3. N. D. Devyatkov, M. B. Golant, and O. V. Betskii, Millimeter Waves and Their Role in Vital Processes [in Russian], Moscow (1991).
4. S. A. Goss, R. L. Johnson, and F. Dunn, J. Acoust. Soc. Amer., **64**, 423-457 (1978).
5. G. D. Ludwig, J. Acoust. Soc. Amer., **22**, 862-866 (1950).
6. D. E. Goldman and T. F. Hueter, J. Acoust. Soc. Amer., **28**, 35-37 (1956).
7. St. Madersbacher, Ch. Kratzik, and M. Marberger, J. Urology, **151**, 399A (1994).
8. E. Ebbini, S. Umemura, M. Ibbini, and C. Cain, IEEE Trans. Ultrason. Ferroelec. Freq. Control, **35**, 561-572 (1988).
9. C. J. Diederich and K. Hynynen, IEEE Trans. Biomed. Eng., **36**, 432-438 (1989).
10. K. B. Ocheltree and L. A. Frizzel, IEEE Trans. Ultrason. Ferroelec. Freq. Control, **36**, 242-248 (1989).
11. G. B. Gentili, F. Gori, and M. Leoncini, IEEE Trans. Biomed. Eng., **38**, 98-103 (1991).
12. L. Segerlind, Application of the Finite-Element Method [Russian translation], Moscow (1979).
13. J. Declou, Finite-Element Method [Russian translation], Moscow (1976).